



Postfach 10 11 61  
69451 Weinheim  
Germany

*Courier services:*  
Boschstraße 12  
69469 Weinheim  
Germany

Tel.: (+49) 6201 606 581

Fax: (+49) 6201 606 510

E-mail: [macromol@wiley-vch.de](mailto:macromol@wiley-vch.de)

WILEY-VCH

---

Dear Author,

**Please correct your galley proofs carefully and return them no more than four days after the page proofs have been received.**

The editors reserve the right to publish your article without your corrections if the proofs do not arrive in time.

Note that the author is liable for damages arising from incorrect statements, including misprints.

Please note any queries that require your attention. These are indicated with a Q in the PDF and a question at the end of the document.

**Please limit corrections to errors already in the text; cost incurred for any further changes or additions will be charged to the author, unless such changes have been agreed upon by the editor.**

**Reprints** may be ordered by filling out the accompanying form.

Return the reprint order form by fax or by e-mail with the corrected proofs, to Wiley-VCH : [macromol@wiley-vch.de](mailto:macromol@wiley-vch.de)

To avoid commonly occurring errors, please ensure that the following important items are correct in your proofs (please note that once your article is published online, no further corrections can be made):

- **Names** of all authors present and spelled correctly
- **Titles** of authors correct (Prof. or Dr. only: please note, Prof. Dr. is not used in the journals)
- **Addresses** and **postcodes** correct
- **E-mail address** of corresponding author correct (current email address)
- **Funding bodies** included and grant numbers accurate
- **Title** of article OK
- All **figures** included
- **Equations** correct (symbols and sub/superscripts)

**Corrections should be made directly in the PDF file using the PDF annotation tools. If you have questions about this, please contact the editorial office. The corrected PDF and any accompanying files should be uploaded to the journal's Editorial Manager site.**

## Author Query Form

# WILEY

Journal MAME  
 Article mame201900353

Dear Author,

During the copyediting of your manuscript the following queries arose.

Please refer to the query reference callout numbers in the page proofs and respond to each by marking the necessary comments using the PDF annotation tools.

Please remember illegible or unclear comments and corrections may delay publication.

Many thanks for your assistance.

Query No.	Description	Remarks
Q1	Please provide a TOC keyword that is suitable for this paper.	
Q2	Please confirm that forenames/given names (blue) and surnames/family names (vermilion) have been identified correctly.	
Q3	Please provide the highest academic title (either Dr. or Prof.) for all authors, where applicable.	
Q4	Please provide postal codes for all affiliations.	
Q5	Please define all acronyms at their first appearance in the abstract, text and table of contents, respectively. Only expanded forms are allowed if the elements are cited only once in the article.	
Q6	Regarding the reference citations present in caption of Figure 1, please provide source line(s) crediting the same in the format: Reproduced with permission. <sup>[Reference number]</sup> Copyright 'year', Publisher name.	
Q7	Please mention ref. [28] in the text.	

**Please confirm that Funding Information has been identified correctly.**

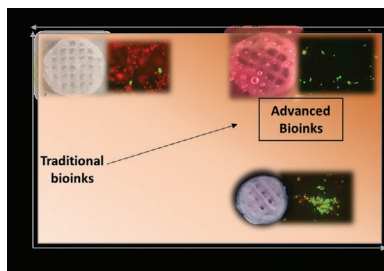
Please confirm that the funding sponsor list below was correctly extracted from your article: that it includes all funders and that the text has been matched to the correct FundRef Registry organization names. If a name was not found in the FundRef registry, it may not be the canonical name form, it may be a program name rather than an organization name, or it may be an organization not yet included in FundRef Registry. If you know of another name form or a parent organization name for a "not found" item on this list below, please share that information.

FundRef Name	FundRef Organization Name
Spanish Ministry of Economy and Competitiveness	
European Regional Development Fund	European Regional Development Fund

xxxx

C. Cofiño, S. Perez-Amodio,  
C. E. Semino, E. Engel,  
M. A. Mateos-Timoneda\* ..... 1900353

**Development of a Self-Assembled Peptide/Methylcellulose-Based Bioink for 3D Bioprinting**



A bioink based on a self-assembled peptide and methylcellulose is developed. The addition of methylcellulose allows the bioprinting of the self-assembled peptide. The bioink exhibits good printability, print fidelity, and biocompatibility. The developed bioink maintains the differentiation potential of the encapsulated cells.

Q1

1  
2  
3  
4  
5  
6  
7  
8  
9  
10  
11  
12  
13  
14  
15  
16  
17  
18  
19  
20  
21  
22  
23  
24  
25  
26  
27  
28  
29  
30  
31  
32  
33  
34  
35  
36  
37  
38  
39  
40  
41  
42  
43  
44  
45  
46  
47  
48  
49  
50  
51  
52  
53  
54  
55  
56  
57  
58  
59

1  
2  
3  
4  
5  
6  
7  
8  
9  
10  
11  
12  
13  
14  
15  
16  
17  
18  
19  
20  
21  
22  
23  
24  
25  
26  
27  
28  
29  
30  
31  
32  
33  
34  
35  
36  
37  
38  
39  
40  
41  
42  
43  
44  
45  
46  
47  
48  
49  
50  
51  
52  
53  
54  
55  
56  
57  
58  
59

UNCORRECTED PROOF

# Development of a Self-Assembled Peptide/Methylcellulose-Based Bioink for 3D Bioprinting

Carla Cofiño, Soledad Perez-Amodio, Carlos E. Semino, Elisabeth Engel,  
and Miguel A. Mateos-Timoneda\*

The introduction of 3D bioprinting to fabricate living constructs with tailored architecture has provided a new paradigm for biofabrication, with the potential to overcome several drawbacks of conventional scaffold-based tissue regeneration strategies. Hydrogel-based materials are suitable candidates regarding cell biocompatibility but often display poor mechanical properties. Self-assembling peptides are a promising source of biomaterials to be used as 3D scaffolds based on their similarity to extracellular matrices (structurally and mechanically). In this study, an advanced bioink for biofabrication is presented based on the optimization of a RAD16-I-based biomaterial. The strategy followed to build 3D predefined structures by 3D printing is based on an enhancement of bioink viscosity by adding methylcellulose (MC) to a RAD16-I solution. The resultant constructs display high shape fidelity and stability and embedded human mesenchymal stem cells present high viability after 7 days of culture. Moreover, cells are also able to differentiate to the adipogenic lineage, suggesting the suitability of this novel biomaterial for soft tissue engineering applications.

## 1. Introduction

The development of novel biomaterials whose properties closely match those needed for a particular application has become increasingly important in advanced tissue engineering.<sup>[1,2]</sup> Self-assembling peptides (SAPs) are a promising class of biomaterials in this field due to their unique properties. This class of 8–32 amino acid long oligopeptides are composed of hydrophilic and hydrophobic amino acid side chains forming a  $\beta$ -sheet structure that can self-assemble when exposed to physiological salt concentrations into a network of interweaving nanofibers of 10 nm diameter, forming hydrogel scaffolds with pores 5–200 nm in diameter and over 99% water content.<sup>[3,4]</sup> The weak interactions formed among peptides, their nanometer size (1000-fold smaller than synthetic polymer micro-

fibers) and mechanical properties are similar to the natural extracellular matrix (ECM), better mimicking the 3D environment found *in vivo*.<sup>[5]</sup> This environment does not contain any specific peptide signaling motif, allowing the addition of specific signaling cues to specifically decorate the environment as desired.<sup>[6]</sup> Among different SAPs,<sup>[7–9]</sup> RAD16-I, commercially available as PuraMatrix, is one of the best candidates for tissue engineering applications.<sup>[10]</sup> RAD16-I consists of 16-amino acid peptide comprised of four repetitive units of Arginine (R), Alanine (A), Aspartic acid (D), and Alanine (A), forming the RADA motif.<sup>[3]</sup> The resultant hydrogel structure of this self-assembling peptide is permeable to small molecules such as gases, nutrients, and growth factors. Moreover, it has been demonstrated that RAD16-I is not immunogenic, does not cause inflammatory reactions nor cytotoxicity<sup>[2]</sup> and has been shown to support attachment, growth, maintenance, and differentiation of a variety of mammalian cells, such as hepatic stem cells, cardiac myocytes, neuronal stem cells, or endothelial cells.<sup>[3]</sup> Therefore, self-assembling peptides can be used for *in vitro* applications for cell 3D culture as well as *in vivo* for tissue regeneration.<sup>[7,11]</sup>

The construction of cell-laden structures able to recapitulate the complexity of native tissues is an engaging strategy to create functional tissue equivalents.<sup>[12,13]</sup> 3D bioprinting is an innovative technology that combines different biomaterials, cells and biological molecules to generate 3D constructs with well-defined architectures based on a layer-by-layer deposition

C. Cofiño, Dr. S. Perez-Amodio, Prof. E. Engel,  
Dr. M. A. Mateos-Timoneda  
Biomaterials for Regenerative Therapies Group  
Institute for Bioengineering of Catalonia (IBEC)  
The Barcelona Institute of Science and Technology  
Barcelona, Spain  
E-mail: mamateos@ibecbarcelona.eu

C. Cofiño, Prof. C. E. Semino  
Department of Bioengineering  
IQS-School of Engineering  
Ramon Llull University  
Barcelona, Spain

Dr. S. Perez-Amodio, Prof. E. Engel, Dr. M. A. Mateos-Timoneda  
CIBER en Bioingeniería  
Biomateriales y Nanomedicina (CIBER-BBN)  
Barcelona, Spain

Dr. S. Perez-Amodio, Prof. E. Engel, Dr. M. A. Mateos-Timoneda  
Department of Material Science and Metallurgical Engineering  
EEBE campus  
Technical University of Catalonia (UPC)  
Barcelona, Spain

The ORCID identification number(s) for the author(s) of this article can be found under <https://doi.org/10.1002/mame.201900353>.

DOI: 10.1002/mame.201900353

process.<sup>[14]</sup> Hydrogel matrices with embedded viable cells, named bioinks, are the preferred building materials in bioprinting due to their instructive and aqueous 3D environment properties, allowing proper conditions for cells.<sup>[14,15]</sup> Although the benefits of bioinks, they trigger some complications regarding their biofabrication, due to their relatively weak mechanical properties.<sup>[16]</sup> In order to build complex and tissue-like structures with high resolution, physical and biological properties must be rigorously adjusted. On the one hand, suitable bioinks should form 3D constructs with high shape fidelity and integrity, by remaining stable for the time of printing procedure and by bearing proper gelation characteristics after being extruded from a nozzle tip and forming solidified filaments mechanically strong enough to support the deposition of the upper layers.<sup>[17]</sup> On the other hand, cell viability is representative of the physiological properties of the bioinks, as they should offer the appropriate microenvironment to support cell survival and activity after printing.<sup>[17,18]</sup> These opposing requirements on the properties of hydrogel materials are reflected in the “biofabrication window” (Figure 1).<sup>[15,19]</sup>

While stiff hydrogels made of high polymer concentrations/high viscosity or high crosslinking densities allow obtaining optimal shape fidelity structures, these dense polymer networks restrict cell migration, growth, and differentiation resulting in low biocompatibilities. On the contrary, soft hydrogels promote adequate cell viability and function, but their low density/low

viscosity leads to poor shape fidelity structures unable to maintain the construct designed. As a result, traditional structures are fabricated with a moderate degree of hydrogel crosslinking densities in order to maintain cell viability. It is desired to shift the bioprinting window and design advanced bioinks with tailored properties that enhance both printability and cell viability.<sup>[15]</sup> In this study, the self-assembling peptide RAD16-I has been proven as a novel biomaterial for 3D bioprinting due to its synthetic origin, properties and high similarity to the natural extracellular matrices. In order to obtain tissue engineering constructs by 3D bioprinting, a strategy to enhance printability has been applied resulting in an optimized RAD16-I/methylcellulose (MC) blend bioink.

## 2. Experimental Section

### 2.1. Bioink Preparation

RAD16-I peptide sterile working solution was prepared from the commercial 1 wt% solution (DB PuraMatrix, Corning). Puramatrix was placed into a conic tube, subsequently in liquid nitrogen until frozen and in the freeze dryer for 72 h. Sucrose 10 wt% (Sigma-Aldrich) was added to the freeze-dried sample to generate a RAD16-I solution at a stock concentration of 3 or 5.5 wt%. Sonication was done when preparing solutions to

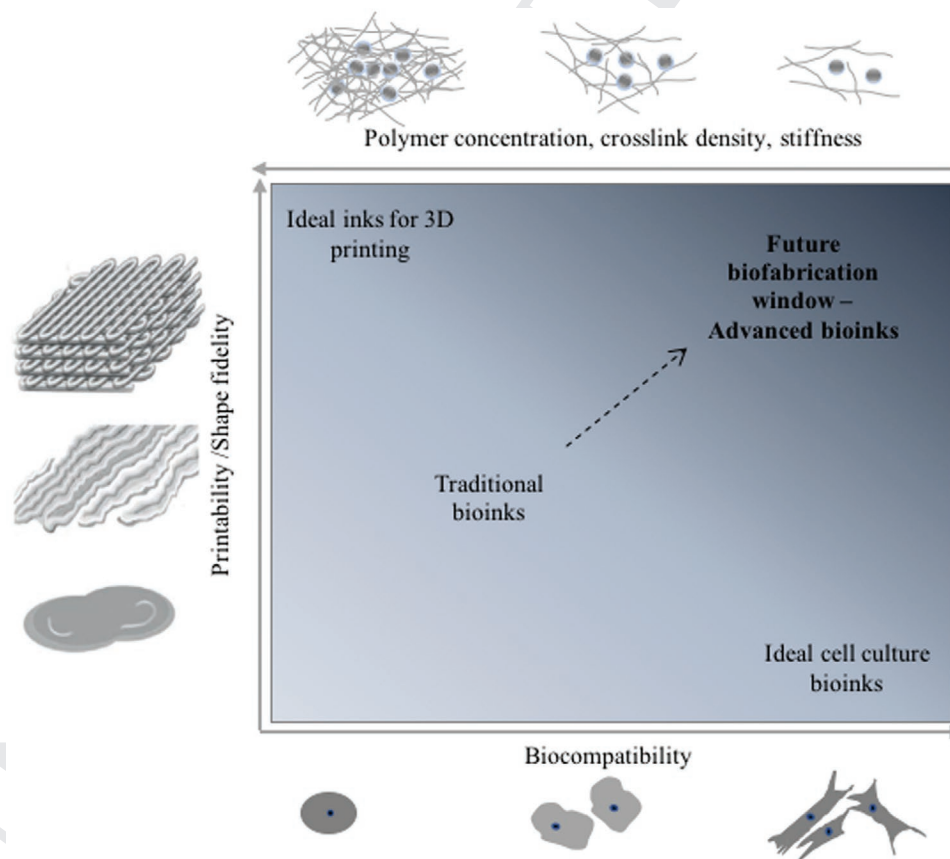


**Figure 1.** Biofabrication window for rational design of bioinks. Future biofabrication window requires advanced bioinks: medium crosslinked hydrogels that provide high shape fidelity with high biocompatibility. Reproduced with permission.<sup>[14,16]</sup>

1 resolubilize the material and facilitate easy handling. Methylcel-  
2 lulose (viscosity: 4000 cPs, MW: 88 kDa, Sigma-Aldrich) (MC)  
3 was sterilized by UV irradiation at 254 nm for 15 min. MC was  
4 prepared in sucrose 10% or PBS (from 1× to 10×) following the  
5 procedure indicated by the manufacturer. After 24 h at 4 °C to  
6 ensure complete dissolution, the final solutions were clear and  
7 transparent. Ratios of RAD:MC 1:2, 3:4 were prepared based  
8 on the dry mass of the compounds adding MC powder to the  
9 RAD16-I 3 wt% solution. For low MC concentrations (from  
10 3% to 1.5%), the plotting material was prepared based on the  
11 volume of each compound. RAD16-I 5.5 wt% was blended with  
12 MC 6.88 wt% to reach a stock concentration of RAD 3.5 + MC  
13 2.5 wt%. The mixtures were thoroughly stirred to homogenize  
14 the solution and stored at 4 °C overnight to ensure complete  
15 swelling of MC. The desired concentration of each compound  
16 was adjusted with the cell suspension or sucrose 10 wt% before  
17 printing. All reagents and materials were sterilized and manip-  
18 ulated under sterile conditions.

## 21 2.2. Viscosity Characterization

22  
23 Viscosity of the peptide solution and RAD:MC blends was  
24 determined at room temperature using an AR 2000ex rheom-  
25 eter (TA Instruments, UK) and a conical plate 20 mm with a  
26 gap of 38 mm. Samples were sonicated for 1 h, one day before  
27 the assay.<sup>[4]</sup> Prior to measure, samples were incubated in a  
28 water bath at 37 °C for 30 min. Viscosity was measured at a  
29 shear rate of 1 s<sup>-1</sup> for 1 min. Viscosity mean values were calcu-  
30 lated at plateau viscosity range ( $n = 3$ ).

## 33 2.3. Circular Dichroism

34  
35 Circular dichroism (CD) studies were performed on a JASCO  
36 J-810 spectropolarimeter at room temperature in a quartz  
37 cuvette (Hellma Standard Cuvette 110 QS) with a pathlength  
38 of 1 mm and in the wavelength range 190–260 nm at a band  
39 width of 1 nm and using three times scans for average. RAD16-  
40 I and MC samples were diluted to get a final concentration in  
41 the RAD+MC blend of 25 and 85 μM, respectively. Solutions  
42 were allowed to equilibrate one day at 4 °C prior to analysis.  
43 Spectra for RAD16-I and MC were also analyzed separately.

## 46 2.4. 3D Printing

47  
48 Hydrogel scaffolds were 3D printed using the 3D Discovery  
49 bioprinter (RegenHU, CH) by dispensing the bioink placed  
50 in a 3 mL syringe through a dosing metal needle of an inner  
51 diameter of 250 or 330 μm (Nordson EFD: precision dispensing  
52 tips, 6.35 mm length). Extrusion parameters for printing were  
53 adjusted by observing the flow of the material out of the needle  
54 in a fixed position. The initial pressure was set when a steady  
55 fiber flow was produced. The feed rate was adjusted based on  
56 the quality and accuracy of the fiber deposition. If the corners  
57 of the crosshatch pattern were not maintained, the speed was  
58 lowered. On the contrary, if too much material was being depos-  
59 ited, non-circular fibers were observed and the pressure and/

or the feed rate were lowered. Hence, pressures applied ranged 1  
from 1.2 to 7 bar and feed rates from 1 to 8 mm s<sup>-1</sup>. The initial 2  
height of the needle above the substrate plate was adjusted by 3  
raising the zero position 2/3 of the needle diameter and it was 4  
further optimized observing the attachment and consistency of 5  
the printed fibers. Note that if air bubbles in the bioink were 6  
formed, samples were centrifuged before printing for 2 min at 7  
25 °C and 1000 rpm. 3D scaffolds were built up layer-by-layer 8  
in a circular crosshatch pattern and after printing the hydrogel 9  
scaffolds were allowed to gel in the flow cabinet with warm 10  
cell culture media for 20 min. At this point, constructs were 11  
manipulated carefully since improper handling before com- 12  
plete crosslinking could break the structure. After this time, 13  
media was replaced with fresh one to eliminate sucrose from 14  
media. At 24 h of incubation, medium was replaced again and 15  
then, every 2–3 days. Vacuum aspiration was not used when 16  
removing the media to avoid direct contact with the sample and 17  
material disruption.

## 21 2.5. Morphological Scaffold Characterization

22  
23 Scanning electron microscopy (SEM) of the 3D bioprinted scaf- 23  
folds was performed. Samples were washed twice with PBS 24  
and dehydrated by a gradation series of ethanol/distilled water 25  
solutions. After critical point drying a carbon coating was per- 26  
formed. Morphological characterization was done with an ultra- 27  
high resolution field SEM Nova NanoSEM 450 FEI microscope. 28  
Image J was used to evaluate fiber diameter and pore size.<sup>[20]</sup> At 29  
least, 20 measurements were taken from ten different images. 30  
The values are reported as value ± SD.

## 34 2.6. 3D Bioprinting with Human Mesenchymal Stem Cells

35  
36 Human mesenchymal stem cells (hMSCs) derived from adi- 36  
pose tissue were used. Cells were expanded in monolayer 37  
culture in Advanced Dulbecco's modified Eagle's medium 38  
(DMEM) supplemented with 10% Fetal Bovine Serum (FBS) 39  
(Sigma-Aldrich), 1% L-Glutamine 100X (Invitrogen), 1% Peni- 40  
cillin/Streptomycin 100X (Invitrogen) and 0,1% Fibroblast 41  
Growth Factor basic (bFGF). Storage conditions were 37 °C 42  
in a 5% CO<sub>2</sub> humidified environment. hMSCs at 80–90% of 43  
confluence were cultured over night with media containing 44  
2% FBS before trypsinization for bioink preparation, adapting 45  
cells to a more stringent environment. Then, a cell suspension 46  
in sucrose 10 wt% was prepared to get a concentration which 47  
corresponds to a final concentration in the bioink solution of 48  
4–1.5 × 10<sup>6</sup> cells mL<sup>-1</sup> (taking into account the volume of cell 49  
suspension to be added to the bioink to get the final concentra- 50  
tion of all compounds). Sucrose 10 wt% was used as it is an 51  
isotonic and non-ionic medium, protecting cells from the acidic 52  
pH of the hydrogel while avoiding peptide gelation during the 53  
mixing process.<sup>[21]</sup> Because cells are in a quite hostile envi- 54  
ronment due to the peptide low pH before medium starts 55  
buffering the suspension, the mixture of cells with the bioink 56  
must be done carefully but quickly at the same time. Hence, 57  
the blending step was performed directly in the 3 mL syringes. 58  
After, bioinks were 3D bioprinted. Printing parameters were set 59

1 following the same premises for 3D printing without cells. For  
2 all the bioprinting assays, a positive control of cells embedded  
3 in the hydrogel solution but not printed was done following  
4 the same procedure except for printing. Negative controls were  
5 produced as cell-laden scaffolds but replacing cell suspension  
6 for sucrose 10 wt%. A heating plate was used at 42 °C during  
7 the printing process in order to induce the gelation of the MC  
8 when prepared in PBS 4X. Treatment of the cell-laden scaffolds  
9 and controls and their 3D culture was conducted in standard  
10 conditions (37 °C, 5% CO<sub>2</sub>) and following the media changes  
11 indicated in Section 2.4.  
12  
13

## 14 2.7. Cell Viability Studies

15  
16 hMSCs viability in the hydrogel was evaluated with the Live/  
17 Dead assay. Samples were gently washed in DPBS 1X (Gibco)  
18 3 times. Then, a solution containing 2 μM Calcein-AM (Life  
19 Technologies) and 2 μM Propidium Iodide (Fluka) was pre-  
20 pared in DPBS 1X. The staining solution was added to the  
21 samples and incubated for 30 min avoiding light. After that  
22 time, samples were extensively rinsed with DPBS (three  
23 washes). Thereafter, images of the constructs were taken using  
24 an inverted fluorescence microscope (Leica DM IL Led). Four  
25 images per scaffold were taken and viability was estimated  
26 using Fiji-ImageJ (National Institutes of Health, NIH). For cell-  
27 laden scaffolds, the Live/Dead assay was performed at 0/4 h of  
28 printing, 1, 3, and 7 days.  
29  
30

## 31 2.8. Adipogenic Differentiation

32  
33 Rat MSCs (rMSCs) at passage 8 and at 90% of confluence were  
34 used. Bioink final concentration was: RAD16-I 2.7% + MC  
35 1.5% + rMSCs 2 × 10<sup>6</sup> cells mL<sup>-1</sup>. After 3D bioprinting the cell-  
36 laden scaffolds, they were incubated over a period of 8 days in  
37 culture medium as follows: for 72 h scaffolds were incubated  
38 with adipogenic induction medium containing Dubelcco's  
39 Modified Eagle Medium (DMEM, Sigma-Aldrich), 10% FBS,  
40 1% L-Glutamine 100X and 1% Penicillin/Streptomycin 100X,  
41 1 μM dexamethasone (Sigma), 0.2 mM indomethacin (Sigma),  
42 5 μg mL<sup>-1</sup> insulin (Sigma), 1 mM 3-Isobutyl-1-methylxanthin  
43 (IBMX, Sigma); then, for 24 h, they were cultured with adipo-  
44 genic maintenance medium containing DMEM base medium,  
45 10% FBS, 1% L-Glutamine 100X, 1% Penicillin/Streptomycin  
46 100X and 0.1 mg mL<sup>-1</sup> insulin; this cycle was repeated three  
47 times. For adipogenic control, non-printed cell-laden hydrogels  
48 were cultivated under the same conditions of the printed scaf-  
49 folds. Negative controls consisted on cell-laden scaffolds cul-  
50 tured with basal medium (DMEM, 10% FBS, 1% L-Glutamine  
51 100X and 1% Penicillin/Streptomycin 100X). Samples were  
52 analyzed for adipogenic differentiation at day 8 of culture for  
53 light microscopy study. Moreover, viability of cell-laden scaf-  
54 folds was checked by Live/Dead staining at day 1, 3, and 7  
55 of culture. For lipid droplets staining, Oil-red O 0.5 wt% re-  
56 agent was used (Sigma-Aldrich). Samples were washed three  
57 times with PBS and fixed for 30 min with 4% paraformalde-  
58 hyde. Afterward, hydrogels were washed twice with PBS and  
59 a staining with Oil-red O (6:4 in water) for 30 min was done.

Then, two more washes with PBS were done. Stained samples  
were imaged with confocal laser scanning microscopy (LSM  
800, Zeiss) using excitation wavelength of 543 nm (619 nm  
emission) for Oil-red O. If crystals of the dye were observed, an  
extra rinse with isopropanol was performed.

## 2.9. Statistical Analysis

Each experiment was performed in three or five replicates (*n* =  
3 or 5). Data are represented as mean and standard deviation of  
the replicates. Statistical significance was assessed performing  
Student's *t*-test using Origin 8.0 Software (OriginLab, USA).

## 3. Results and Discussion

### 3.1. Bioink Characterization for 3D Bioprinting

#### 3.1.1. Improvement of RAD16-I Printability

A bioink formulation should be able to be deposited in succes-  
sive layers without collapsing when printed in air.<sup>[22]</sup> In order to  
produce biological constructs with well-defined geometry and  
integrity, RAD16-I (3% w/v) was 3D printed and the resultant  
structure was unable to maintain the designed pattern due to  
the fluxion of the material because of the low viscosity of the  
SAP despite increasing its concentration (Table 1).

Then, to improve the shape fidelity of RAD16-I, and con-  
sequently the viscosity of the bioink,<sup>[23]</sup> methylcellulose (MC)  
was used as a reinforcer material and thickening agent. This  
biopolymer was chosen as it is biocompatible and biodegrad-  
able and its gelling capacities can be tailored by its concentra-  
tion and molecular weight and influenced by the presence of  
salts.<sup>[24–26]</sup> In order to set which concentration of methylcellu-  
lose was the most appropriated to blend with the peptide solu-  
tion, three bioinks were formulated and 3D-printed. Ratios of  
RAD:MC (RAD16-I:MC) were tested (1:1, 1:2, 3:4) (Figure 2,  
Table 2).

MC allows the precise deposition of the bioink material  
(Figure 2a,b) and a concentration of 4 wt% mixed homogene-  
ously with a 3 wt% peptide solution allows plotting scaffolds  
of high shape fidelity, showing a strand width of 396 ± 37 μm,  
closer to the theoretical one (330 μm) (Figure 2d). Rheological  
studies of the chosen bioink confirmed that MC improved  
significantly the viscosity of the solution. At low shear rates  
(1 s<sup>-1</sup>) viscosity of the pregel solution of RAD16-I 3% + MC

**Table 1.** Viscosities of different bioink solutions before gelation.

Material [wt%]	Viscosity [Pa s] <sup>a)</sup>
RAD16-I 1%	4
RAD16-I 3%	20
RAD16-I 3% + MC 2%	256
RAD16-I 3% + MC 4%	290

<sup>a)</sup>Viscosity calculated at 1 s<sup>-1</sup> shear rate.

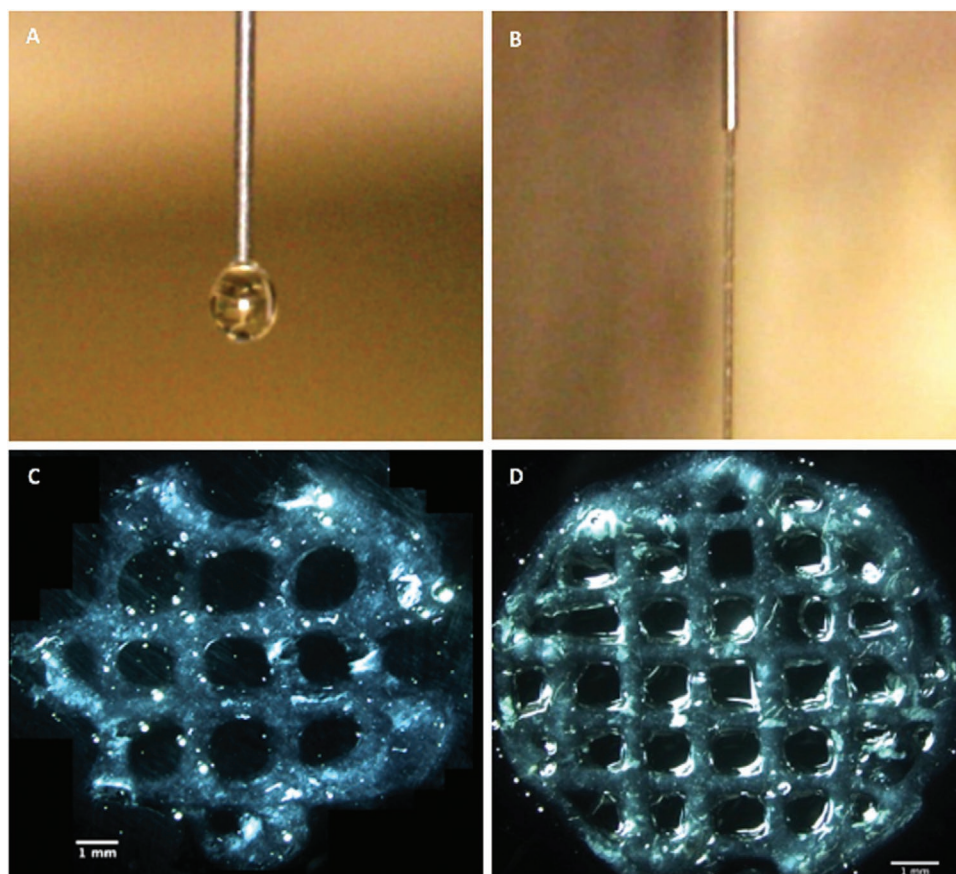


**Figure 2.** Printability studies to set the adequate methylcellulose (MC) concentration to blend with RAD16-I 3 wt%. A) Air extrusion of RAD16-I 3%. B) Air extrusion of RAD16-I 3% + MC 6% solution. C, D) Stereomicroscopy images of scaffolds fabricated with RAD16-I 3% + MC 3% and RAD16-I 3% + MC 4%, respectively (scale bar 1 mm).

4% was 14-fold higher than the 3% peptide solution (Table 1). Therefore, the viscosity of the bioink solution mainly determines the overall performance of the fiber deposition during the printing process. Viscoelastic properties were indicative of the relative mechanical stiffness of the peptides in the preassembled versus the assembled peptides. The linear viscoelastic region, where both  $G'$  and  $G''$  moduli were constant,<sup>[27]</sup> was 0.01 (dimensionless) (Figure S1, Supporting Information). Despite the fact that both RAD16-I and RAD16-I + MC solutions presented a gel-like behavior with  $G' > G''$  constant along the range of frequencies tested, the RAD16-I+MC solution showed a higher modulus ( $G'$  and  $G''$ ) than the peptide solution (Figure S2, Supporting Information). After

**Table 2.** Printing parameters used for 3D-print the different blended hydrogel scaffolds.

Printing parameters <sup>a)</sup>	Bioink solution		
	RAD 3% + MC 6%	RAD3% + MC 3%	RAD3% + MC 4%
Pressure [bar]	6–7	1.2–1.4	4
Feed rate [mm s <sup>-1</sup> ]	1	6–8	5

<sup>a)</sup> Needle inner diameter: 0.25 mm.

crosslinking the solutions, the modulus showed an enhancement of 100-fold for RAD16-I solution and 20-fold for the composite solution, indicating a significant increase of gel strength (Figure S2, Supporting Information). Moreover, each gel reached equilibrium with the buffer solution, maintained stable rheological properties with time and no significant differences were observed between RAD16-I and with the addition of MC, indicating that the crosslinking of the peptide was not altered (Figure S3, Supporting Information). Additionally, circular dichroism (Figure 3) studies proved that the addition of MC did not interfere in the  $\beta$ -sheet structure of the peptide and thus it could self-assembled to form nanofibers.

Moreover, SEM of the hydrogel scaffolds revealed that the structure was presented as a flat membrane at low magnifications (Figure 4a), but the membrane appears formed of interwoven individual filaments when observed at higher magnifications (Figure 4b). The mean fiber diameter of the nanofibers was  $34 \pm 7.25$  nm and the pore size of the interwoven structure  $158 \pm 59.76$  nm, similar to theoretical values of RAD16-I nanofibers (nanofibers of 10–20 nm in diameter and pore size between 5 and 200 nm).<sup>[4]</sup> Therefore, SEM analysis confirmed that the resulting scaffolds presented a porous surface, combining both micro and nanoporosity, allowing biomolecular diffusion and mimicry to the ECM.<sup>[27]</sup>



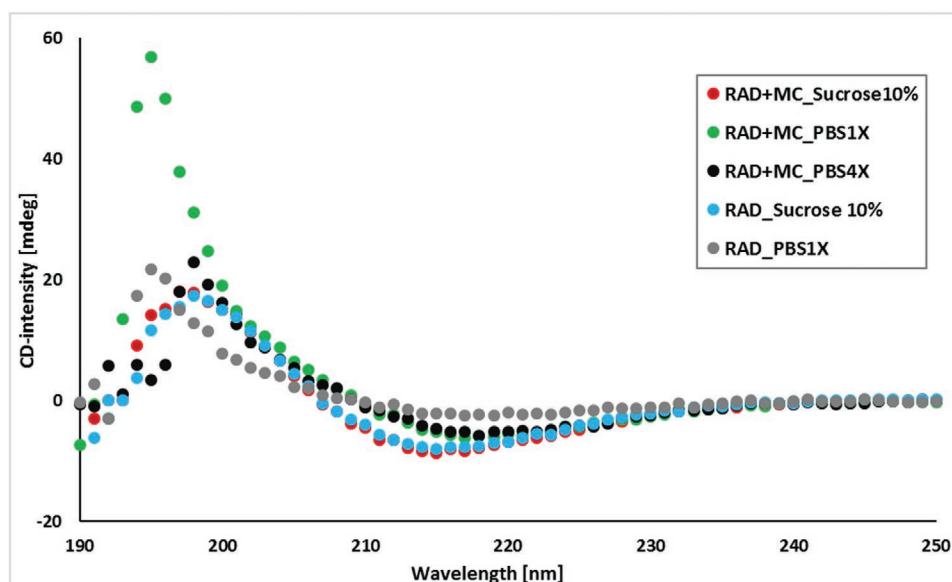


**Figure 3.** Circular dichroism spectra of RAD16-I (RAD) dissolved in sucrose 10 wt% or PBS 1X and RAD + MC dissolved in sucrose 10 wt%, PBS 1X, or PBS 4X.

### 3.1.2. Cell Viability within the Bioink

It is known that SAPs are characterized by exhibiting a low pH, which implies working quickly when encapsulating cells within the prehydrogel solution in order to minimize the time that cells are in this hostile environment. Therefore, the encapsulation step is the main critical point of the whole process and where cell viability is more affected.<sup>[29]</sup> The RAD16-I 3% solution exhibits a pH of 1, and the addition of MC did not produce an increase of pH. Thus, when the RAD16-I 3% + MC 4% was first used to encapsulate quickly the human mesenchymal stem cells (hMSCs) at a final concentration of  $4 \times 10^6$  cells mL<sup>-1</sup> and bioprinted, the scaffold maintained high shape fidelity but the resultant cell viability was significantly low (Figure 5).

This low cell viability could be explained either by the increment of the printing pressure (5 bar) or because of the time cells were in contact with the low pH of the peptide solution before reaching physiological pH. MC was dissolved in different PBS concentrations in order to allow the diffusion of PBS in the MC to the RAD16-I solution once blended and stabilized. Here, two main factors were considered. On the one hand, if PBS could increase the pH of the pregel solution, this would imply that the peptide solution would partially cross-link. Then, the PBS concentration should increase the pH but to a point where the structure of the peptide was maintained enough to be 3D printed and not broken (for the weak interactions that form the hydrogel). On the other hand, due to the increment in the pressure for extrusion observed during

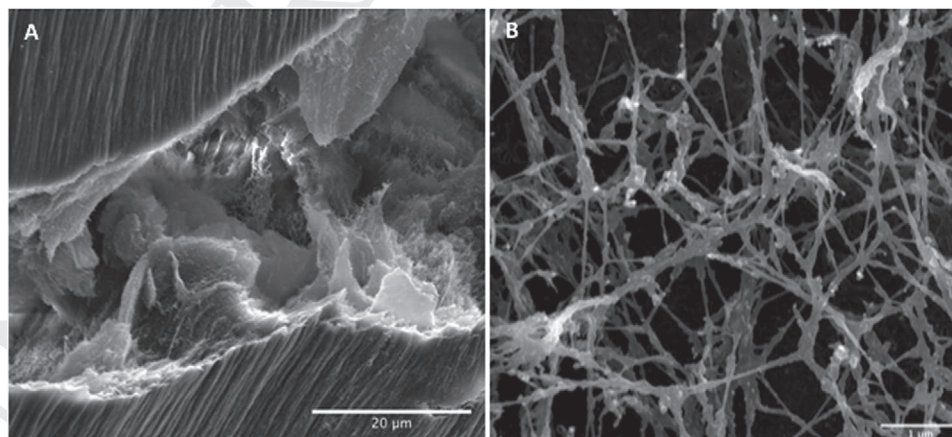


**Figure 4.** SEM images of RAD16-I 3% + MC 4% hydrogel scaffolds at different magnifications: A) 5000X (scale bar 20 μm) and B) 50 000X (scale bar 1 μm).

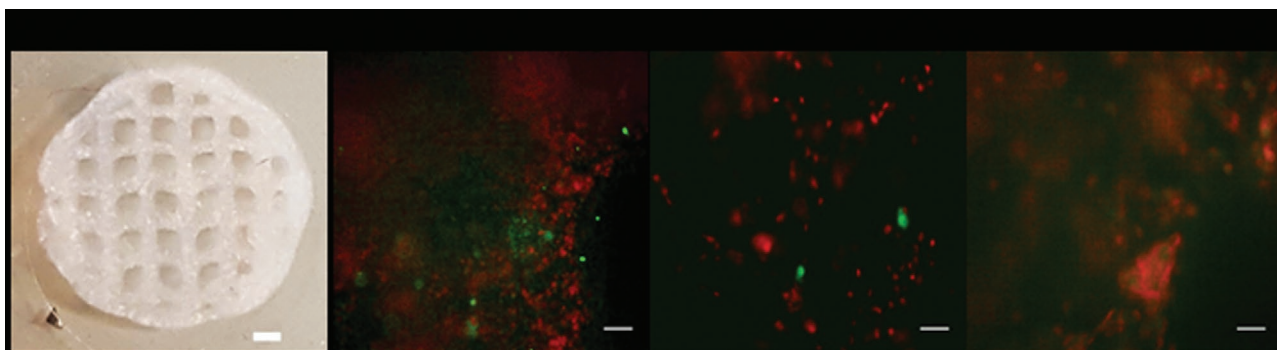


**Figure 5.** Assessment of RAD16-I 3% + MC 4% hydrogel scaffolds biofabrication. A) Scaffold 3D printed: 5 mm radius, 1.5 strand distance, 4 layers printed (Scale bar: 1 mm). B) Viability of cells embedded in the printed scaffolds at 0 h, 1, and 3 days after printing (scale bar: 500  $\mu\text{m}$ ). Green: live cells; red: dead cells.

the first bioprinting experiment and considered that the addition of PBS to the MC could reinforce the pregel solution, it was decided to reduce to 2 wt% the concentration of MC. Thereafter, different concentrations of PBS (from 1X to 10X) were used to dissolve MC and then MC was blended with RAD16-I to obtain a final concentration of RAD16-I 3% + MC 2% (wt). The pH of each solution was measured (Figure S4, Supporting Information) and it was observed that PBS 4X was the most appropriate to be used since it increased the pH of the solution to 2.5, as the pH of a typical working concentration of RAD16-I (0.5% w/v). Cell viability assays confirmed that RAD16-I 3% + MC 2% (MC in PBS 4X) could maintain a moderate cell viability in the pregel solution for 10 min before reaching neutrality, compared to the low cell viability obtained without the MC dissolved in PBS (Figure S5, Supporting Information).

### 3.2. Bioink Optimization for 3D Bioprinting

Rheological analysis confirmed that despite reducing the MC concentration, it was still able to increase the viscosity of the pregel solution up to 13-fold higher than the peptide solution viscosity (Table 1). After some 3D-bioprinting analysis, it was found that the best cell-laden scaffolds showing both high shape fidelity and high cell viability were produced when the bioink formulation was made of RAD16-I 2.7% + MC 1.5% (MC in PBS 4X) with hMSCs at a final concentration of  $1.5 \times 10^6$  cells  $\text{mL}^{-1}$ . This reduction of concentrations might allow higher permeability of nutrients and oxygen within the printed scaffolds while the partially low crosslinking favored the maintenance of the pregel viscosity. The cell-laden scaffolds were printed with an extrusion pressure of 0.6–1 bar, a feed rate of 8–9  $\text{mm s}^{-1}$  and with a needle of 330  $\mu\text{m}$  inner diameter. Additionally, the surface of the wells where the strands were being deposited was previously equilibrated with cell culture media to induce quickly a physiological environment. Moreover, since it has been reported that the addition of PBS decreases the gelling temperature of MC,<sup>[24]</sup> a heater plate at 42  $^{\circ}\text{C}$  was used during printing in order to induce its gelation and reinforce the scaffold structure once deposited on the well plate. The resulting cell-laden scaffolds exhibited

good printability (Figure 6a) with a strand width of  $430 \mu\text{m} \pm 66 \mu\text{m}$ , closer to the theoretical one (330  $\mu\text{m}$ ). At 4 h, 1, 3, and 7 days of culture after printing, cell viability was evaluated and quantified (Figure 6b,c). It can be observed that cells were also homogeneously distributed within the scaffold and that at day 3 of culture they exhibited both round and rudimentary filopodia morphologies. Immunostaining of embedded cells at day 2 of culture confirmed this morphology (Figure S6, Supporting Information).

Viability of cells embedded in the hydrogel but not printed was also monitored as a positive control. On the one hand, right after printing (4 h), a great number of living but also of dead cells were observed, leading to a viability of around 55%. Cells not being printed exhibited a cell viability about 70%. Then, the reduction of viability at 4 h could be associated with the printing process. At day 1 of culture, cells recovered from the shear forces applied to them during printing and showed a viability of approximately 65%, corresponding with the viability at day 1 of non-printed cells. Therefore, at day 1, cells were likely being adapted to the new 3D environment and recovering from the stresses applied during bioink manipulation. On the other hand, at days 3 and 7 of culture, cell viability started to increase in the non-printed embedded cells but not in the case of the cells embedded in the scaffolds. In this case, cell viability at day 3 was still similar to day 1 but after 7 days of culture, it increased to  $\approx 80\%$ , similar to the viability of the non-printed cells. For example, it was useful to compare these results with other cell viability studies of cell-laden hydrogels printed. It was observed that after 7 days of culture similar results were achieved with a cell viability of around 80%.<sup>[30]</sup> Other studies obtained opposite results, meaning that the viability of cells embedded and printed was higher the first day after printed than after 7 days of culture.<sup>[22]</sup> Then, this could indicate that the RAD16-I+MC hydrogel used is suitable for long-term cell studies since it allows maintaining both scaffold structure and cell viability during time, confirming the stability of the SAP. Since RAD16-I presents a low biodegradation<sup>[29]</sup> in contrast to MC, cells would be able to proliferate and generate their own ECM, replacing first the MC and then the RAD being degraded. Nevertheless, more studies should be done in order to assess for how long the scaffold structure can be maintained. As a result, when MC was dissolved

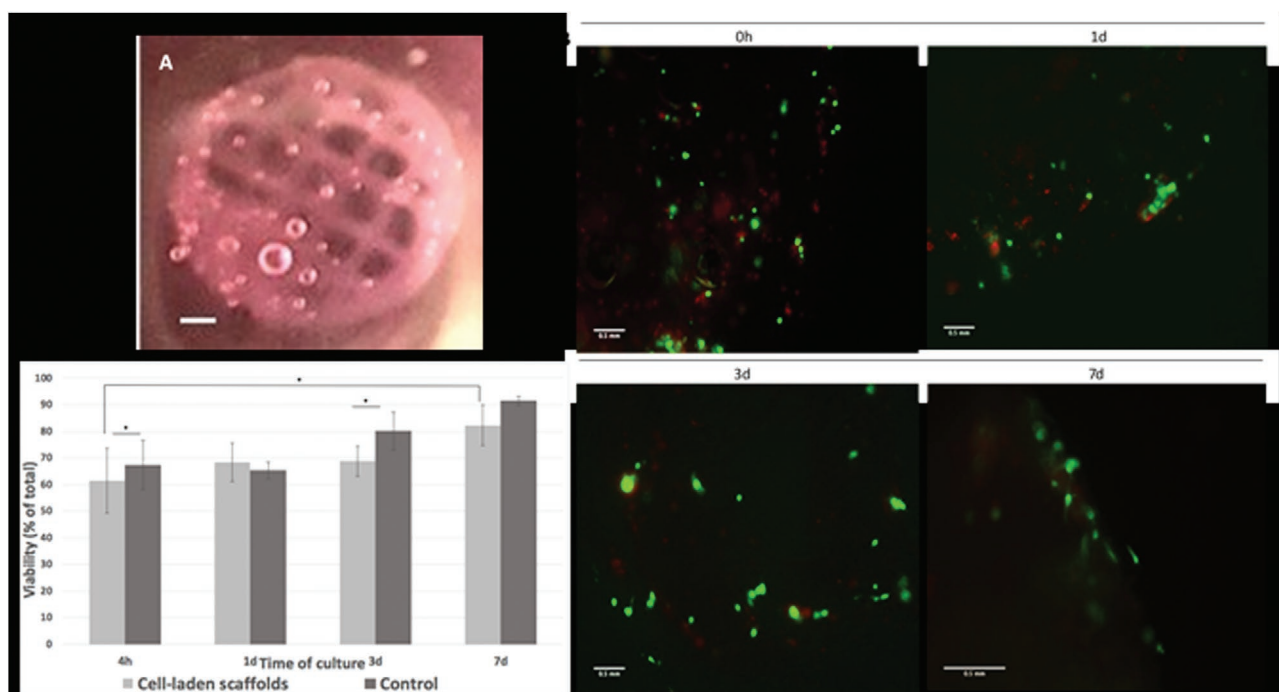


**Figure 6.** Optimized bioink for 3D bioprinting consisting on RAD16-I 2.7 wt% + MC 1.5 wt% + hMSC  $1.5 \cdot 10^6$  cells  $\text{mL}^{-1}$ . A) 3D bioprinted scaffold in cell culture media with 4 mm radius, strand distance of 1.5 mm, and 2 layers height (scale bar 1 mm). B) Viability images of cells embedded within the scaffolds at 4 h, 1, 3, and 7 days (d) of culture (scale bar 0.5 mm). C) Viability quantification of embedded cells in the 3D bioprinted scaffold compared with the embedded cells non printed (control). Green: live cells; Red: dead cells.

in PBS 4X and the concentrations of both components of the bioink were slightly reduced, cell-laden scaffolds could be printed with both good shape fidelity and relatively high percentage of cell viability.

### 3.3. rMSCs Adipogenic Differentiation

Adipogenic differentiation of rat mesenchymal stem cells (rMSCs) embedded within the RAD 2.7% + MC 1.5% 3D-bioprinted scaffolds was evaluated by Oil-red O staining of lipid vesicles at day 8 of culture with or without adipogenic media.<sup>[31]</sup> rMSC were used in this assay as they are easier to handle and differentiate more quickly to the adipogenic lineage than hMSCs. Results obtained from the Oil-red O staining indicated that rMSCs were able to differentiate to adipogenic lineage (Figure 7) since lipid droplets inside the adipogenically induced cells were found after 8 days of culture.<sup>[32]</sup>

## 4. Conclusions

In this study, a novel bioink of RAD16-I and methylcellulose has been suggested as a candidate biomaterial for 3D bioprinting as a strategy to overcome the main bottleneck that biofabrication must face: the development of advanced bioinks that combine both high printability and biocompatibility. The optimization of the bioink formulation and the printing process lead to the construction of stable 3D scaffolds of well-defined

geometry, high shape fidelity and cell viability after 7 days of culture. Adipogenic differentiation was a proof of concept to show the potential of this bioink for soft tissue engineering systems. The bioink presented here is thought to be a potential

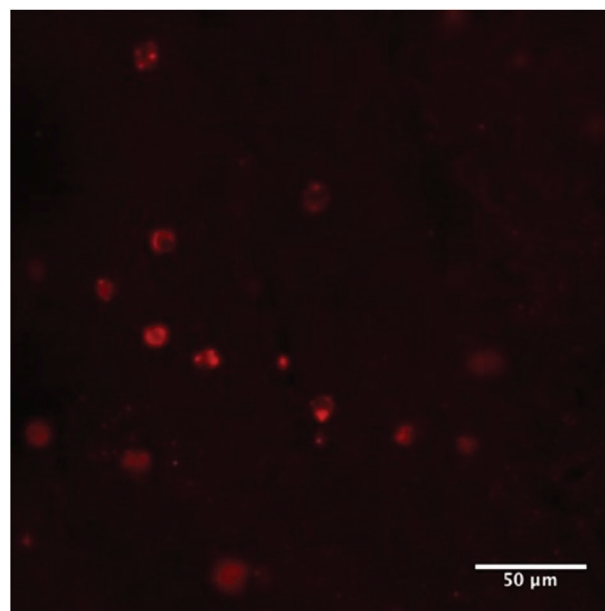


**Figure 7.** Oil-red O staining of adipogenically induced rMSCs at day 8 of culture. Red: lipid droplets in fat vacuoles (scale bar 50 μm).

1 biomaterial for advanced tissue engineering applications con-  
2 sidering the advantages that offer the RAD16-I peptide and its  
3 versatility to be easily blended with CM.

## 6 Supporting Information

7 Supporting Information is available from the Wiley Online Library or  
8 from the author.

## 12 Acknowledgements

13 Part of this work was supported by the Spanish Ministry of Economy and  
14 Competitiveness through the project [MAT2015-68906-R] (MINECO/  
15 FEDER) and CERCA Programme/Generalitat de Catalunya. This work has  
16 been developed in the context of QuiroFAM project (COMRD116-1-0011)  
17 with the support of ACCIÓ (Catalonia Trade & Investment; Generalitat  
18 de Catalunya) and the European Community under the Catalonian ERDF  
19 operational program (European Regional Development Fund) 2014–  
20 2020. Part of the work has been performed at the ICTS “NANBIOSIS,”  
21 Unit 5 of CIBER in Bioengineering, Biomaterials & Nanomedicine  
22 (CIBER-BBN) at IBEC.

## 24 Conflict of Interest

25 The authors declare no conflict of interest.

## 28 Keywords

29 3D bioprinting, biofabrication, bioink, self-assembling peptides, tissue  
30 engineering

Received: May 31, 2019  
Revised: July 1, 2019  
Published online:

- 31 [1] S. Zhang, T. C. Holmes, C. M. DiPersio, R. O. Hynes, X. Su, A. Rich,  
32 *Biomaterials* **1995**, *16*, 1385.  
33 [2] S. Zhang, Z. Zhao, L. Spirio, *Scaffolding Tissue Engineering*, CRC  
34 Press, Boca Raton, FL **2013**.  
35 [3] A. L. Sieminski, C. E. Semino, H. Gong, R. D. Kamm, *J. Biomed.*  
36 *Mater. Res., Part A* **2008**, *87A*, 494.  
37 [4] E. Genové, C. Shen, S. Zhang, C. E. Semino, *Biomaterials* **2005**, *26*,  
38 3341.

- [5] C. Castells-Sala, L. Recha-Sancho, A. Lluçà-Valldeperas, C. Soler-  
1 Botija, A. Bayes-Genis, C. E. Semino, *Tissue Eng., Part C* **2016**, *22*, 113.  
2 [6] C. E. Semino, *J. Biomed. Biotechnol.* **2003**, *2003*, 164.  
3 [7] M. Zelzer, R. V. Ulijn, *Chem. Soc. Rev.* **2010**, *39*, 3351.  
4 [8] K. Tao, A. Levin, L. Adler-Abramovich, E. Gazit, *Chem. Soc. Rev.*  
5 **2016**, *45*, 3935.  
6 [9] L. Adler-Abramovich, E. Gazit, *Chem. Soc. Rev.* **2014**, *43*, 6881.  
7 [10] C. E. Semino, *J. Dent. Res.* **2008**, *87*, 606.  
8 [11] Z. Q. Yu, Z. Cai, Q. L. Chen, M. H. Liu, L. Ye, J. Y. Ren, W. Z. Liao,  
9 S. W. Liu, *Biomater. Sci.* **2016**, *4*, 365.  
10 [12] T. Jungst, W. Smolan, K. Schacht, T. Scheibel, J. Groll, *Chem. Rev.*  
11 **2016**, *116*, 1496.  
12 [13] G. Gao, B. S. Kim, J. Jang, D.-W. Cho, *ACS Biomater. Sci. Eng.* **2019**,  
13 *5*, 1150.  
14 [14] R. Levato, J. Visser, J. A. Planell, E. Engel, J. Malda, M. A. Mateos-  
15 Timoneda, *Biofabrication* **2014**, *6*, 035020.  
16 [15] J. Malda, J. Visser, F. P. Melchels, T. Jungst, W. E. Hennink, W. J.  
17 A. Dhert, J. Groll, D. W. Hutmacher, *Adv. Mater.* **2013**, *25*, 5011.  
18 [16] Y. B. Kim, H. Lee, G.-H. Yang, C. H. Choi, D. Lee, H. Hwang,  
19 W.-K. Jung, H. Yoon, G. H. Kim, *J. Colloid Interface Sci.* **2016**, *461*, 359.  
20 [17] L. Ouyang, R. Yao, Y. Zhao, W. Sun, *Biofabrication* **2016**, *8*, 035020.  
21 [18] N. Paxton, W. Smolan, T. Böck, F. Melchels, J. Groll, T. Jungst, *Bio-*  
22 *fabrication* **2017**, *9*, 044107.  
23 [19] D. Chimene, K. K. Lennox, R. R. Kaunas, A. K. Gaharwar, *Ann.*  
24 *Biomed. Eng.* **2016**, *44*, 2090.  
25 [20] C. A. Schneider, W. S. Rasband, K. W. Eliceiri, *Nat. Methods* **2012**,  
26 *9*, 671.  
27 [21] S. Singh, *Biotechnology Thesis*, Chalmers University of Technology  
28 (Sweden), **2014**.  
29 [22] Y. He, F. Yang, H. Zhao, Q. Gao, B. Xia, J. Fu, *Sci. Rep.* **2016**, *6*,  
30 29977.  
31 [23] K. Hölzl, S. Lin, L. Tytgat, S. van Vlierberge, L. Gu, A. Ovsianikov,  
32 *Biofabrication* **2016**, *8*, 032002.  
33 [24] P. Zheng, L. Li, X. Hu, X. Zhao, *J. Polym. Sci., Part B: Polym. Phys.*  
34 **2004**, *42*, 1849.  
35 [25] R. J. Leddon, *Manuf. Chem. Aerosol News* **1948**, *19*, 287.  
36 [26] N. Law, B. Doney, H. Glover, Y. Qin, Z. M. Aman, T. B. Sercombe,  
37 L. J. Liew, R. J. Dilley, B. J. Doyle, *J. Mech. Behav. Biomed. Mater.*  
38 **2018**, *77*, 389.  
39 [27] G. A. Schramm, *A Practical Approach to Rheology and Rheometry*,  
40 ThermoHaake, Karlsruhe, Germany **1994**.  
41 [28] E. C. Wu, S. Zhang, C. A. E. Hauser, *Adv. Funct. Mater.* **2012**, *22*, 456.  
42 [29] F. Berthiaume, J. R. Morgan, *Methods in Bioengineering: 3D Tissue*  
43 *Engineering*, Artech House, Norwood, MA **2012**.  
44 [30] K. Markstedt, A. Mantas, I. Tournier, H. Martínez Ávila, D. Hägg,  
45 P. Gatenholm, *Biomacromolecules* **2015**, *16*, 1489.  
46 [31] C. A. van Blitterswijk, J. de Boer, *Tissue Engineering*, Elsevier,  
47 London, UK **2002**.  
48 [32] A. Aldridge, D. Kouroupis, S. Churchman, A. English, E. Ingham,  
49 E. Jones, *Cytotherapy* **2013**, *15*, 89.

# Macromolecular Materials and Engineering



Editorial Office:  
Wiley-VCH Verlag  
Boschstraße 12, 69469 Weinheim  
Germany  
Tel.: +49 (0) 6201 – 606 – 581  
Fax: +49 (0) 6201 – 606 – 510  
Email: macromol@wiley-vch.de

## Reprint Order Form

Manuscript No.: \_\_\_\_\_  
Customer No.: (if available) \_\_\_\_\_  
Purchase Order No.: \_\_\_\_\_  
Author: \_\_\_\_\_

**Charges for Reprints in Euro (excl. VAT), prices are subject to change. Minimum order 50 copies.**

No. of pages	50 copies	100 copies	150 copies	200 copies	300 copies	500 copies
1–4	345,—	395,—	425,—	445,—	548,—	752,—
5–8	490,—	573,—	608,—	636,—	784,—	1077,—
9–12	640,—	739,—	786,—	824,—	1016,—	1396,—
13–16	780,—	900,—	958,—	1004,—	1237,—	1701,—
17–20	930,—	1070,—	1138,—	1196,—	1489,—	2022,—
every additional 4 pages	147,—	169,—	175,—	188,—	231,—	315,—

**Information regarding VAT:** The charges for publication of *cover pictures /reprints/issues/poster/Video abstracts/* are considered to be “supply of services” and therefore subject to German VAT. However, if you are an institutional customer outside Germany, the tax can be waived if you provide us with the valid VAT number of your company. Non-EU customers may have a VAT number starting with “EU” instead of their country code, if they are registered with the EU tax authorities. If you do not have a valid EU VAT number and you are a taxable person doing business in a non-EU country, please provide a certification from your local tax authorities confirming that you are a taxable person under local tax law. Please note that the certification must confirm that you are a taxable person and are conducting an economic activity in your country. **Note:** certifications confirming that you are a tax-exempt legal body (non-profit organization, public body, school, political party, etc.) in your country do not exempt you from paying German VAT.

Please send me send bill me for

- no. of reprints
- high-resolution PDF file (330 Euro excl. VAT)  
E-mail address: \_\_\_\_\_

❖ Special Offer:

If you order 200 or more reprints you will get  
a PDF file for half price.

*Please note: It is not permitted to present the PDF file on  
the internet or on company homepages.*

**Cover Posters** (prices excl. VAT)

Posters of published covers are available in two sizes:

- DinA2 42 x 60 cm / 17 x 24in (one copy: 39 Euro)
- DinA1 60 x 84 cm / 24 x 33in (one copy: 49 Euro)

**Postage for shipping** (prices excl. VAT)

overseas +25 Euro  
within Europe +15 Euro

VAT number: \_\_\_\_\_

Mail reprints / copies of the issue to:

\_\_\_\_\_  
\_\_\_\_\_  
\_\_\_\_\_  
\_\_\_\_\_

Send bill to:

\_\_\_\_\_  
\_\_\_\_\_  
\_\_\_\_\_

I will pay by bank transfer

I will pay by credit card

**VISA, Mastercard and AMERICAN EXPRESS**

For your security please use this link (Credit Card  
Token Generator) to create a secure code Credit  
Card Token and include this number in the form  
instead of the credit card data. Click here:

[https://www.wiley-vch.de/editorial\\_production/index.php](https://www.wiley-vch.de/editorial_production/index.php)

**CREDIT CARD TOKEN NUMBER**

						V													
--	--	--	--	--	--	---	--	--	--	--	--	--	--	--	--	--	--	--	--

Date, Signature \_\_\_\_\_